



## PAPER

## The envelope Hamiltonian for electron interaction with ultrashort pulses

## OPEN ACCESS

## RECEIVED

10 February 2015

## REVISED

12 May 2015

## ACCEPTED FOR PUBLICATION

2 June 2015

## PUBLISHED

3 July 2015

Koudai Toyota, Ulf Saalmann and Jan M Rost

Max Planck Institute for the Physics of Complex Systems, Nöthnitzer Straße 38, D-01187 Dresden, Germany

E-mail: [us@pks.mpg.de](mailto:us@pks.mpg.de)**Keywords:** photo-ionization, free-electrons laser, Floquet expansion, light–matter coupling

Content from this work may be used under the terms of the [Creative Commons Attribution 3.0 licence](https://creativecommons.org/licenses/by/3.0/).

Any further distribution of this work must maintain attribution to the author(s) and the title of the work, journal citation and DOI.

**Abstract**

For ultrashort VUV pulses with a pulse length comparable to the orbital time of the bound electrons they couple to, we propose a simplified envelope Hamiltonian. It is based on the Kramers–Henneberger representation in connection with a Floquet expansion of the strong-field dynamics but keeps the time dependence of the pulse envelope explicit. Thereby, the envelope Hamiltonian captures the essence of the physics—light-induced shifts of bound states, single-photon absorption, and non-adiabatic electronic transitions. It delivers quantitatively accurate ionization dynamics and allows for a physical insight into the processes occurring. Its minimal requirements for construction in terms of laser parameters make it ideally suited for a large class of atomic and molecular problems.

**1. Introduction**

Interaction of strong light fields with bound electrons continues to produce new experimental phenomena while theory is looking for appropriate approximations since this dynamics, even for a single active electron, is not analytically solvable. Nevertheless, the interaction with femtosecond pulses in the infrared domain is by now well understood as long as a single-active-electron description is suitable. More recently, the domain of slow photo-electrons has become a centre of attention through the discovery of substantial photo-electron yields with a couple of eV kinetic energy in atoms and molecules exposed to mid-infrared laser fields [1–4].

In parallel advanced optical techniques allow for the generation of attosecond light pulses so short that their pulse duration  $T$  can reach the period of a bound electron  $T_\nu$  they couple to. Also here, in simulations a surprisingly large yield of low energy electrons was found [5, 6] despite the fact that the carrier frequency  $\omega$  was high enough to elevate the photo electrons well into the continuum by single-photon ionization (SPI). However, dynamics gets involved for this regime of light–matter coupling, characterized by the hierarchy of time scales

$$T \sim T_\nu > T_\omega \quad (1)$$

with  $T_\omega = 2\pi/\omega$ , since the time envelope of the laser pulse with length  $T$  becomes dynamically important. This is the reason why so far electron dynamics in this regime [7] could only be described fully numerically although the dominant single-photon absorption suggests the possibility for a suitable perturbation theory.

In the following we will formulate the basis for such a perturbative approach by introducing the envelope Hamiltonian which condenses possible non-adiabatic electron transitions due to the short pulse envelope into a single matrix element with zero-photon absorption similarly to the matrix elements for  $n$ -photon transitions. Solved fully numerically, the envelope Hamiltonian captures accurately the ionization dynamics as will be demonstrated in comparison with the numerical solution of the time-dependent Schrödinger equation for two examples, as will be detailed in section 2. Moreover, for suitable parameters, the envelope Hamiltonian also suggests itself for perturbative treatment developed in section 3, in which  $n$ -photon transitions (including zero-photon transitions !) appear as matrix elements of solutions for the system time-averaged over an optical cycle, as will be shown in section 4.

## 2. The envelope Hamiltonian $\mathcal{H}_2$

### 2.1. Cycle-averaged time-dependent Kramers–Henneberger (KH) potentials

We use atomic units unless stated otherwise and start from the Hamiltonian in the KH frame [8]

$$\mathcal{H} = -\frac{1}{2}\nabla^2 + V(\mathbf{r} + \mathbf{e}_x x_\omega(t)), \quad (2)$$

where  $V$  is the potential in which the electron is bound and  $x_\omega$  is the classical quiver position in a linearly polarized laser field along  $x$ , marked by the unit vector  $\mathbf{e}_x$ . The KH frame has been extensively used in the context of stabilization [9, 10] and recently to interpret strong-field photo-ionization data of atoms [11].

To facilitate the analytical derivations of the cycle-averaged time-dependent KH potentials, ultimately leading to the envelope Hamiltonian, we define the laser field  $F(t)$  in terms of the quiver amplitude entering (2),

$$F(t) = -\frac{d^2 x_\omega}{dt^2}, \quad (3)$$

with  $x_\omega$  specified analytically as

$$x_\omega(t) = \alpha(t) \cos(\omega t + \delta), \quad (4a)$$

$$\alpha(t) \equiv \alpha_0 e^{-4 \ln^2(t/T)^2}. \quad (4b)$$

Thus  $F(t)$  describes a finite pulse with duration  $T$  (full width at half maximum), and it represents a proper electromagnetic pulse [12] with vanishing dc component  $\int dt F(t) = dx_\omega(t)/dt|_{-\infty}^{+\infty} = 0$  and vanishing displacement  $\int dt A(t) = x_\omega(t)|_{-\infty}^{+\infty} = 0$ . For the pulse to remain in the non-relativistic domain, we characterize it with the maximum field strength  $F(0) = F_0 \cos \delta$  which leads to the prefactor

$$\alpha_0 = \frac{F_0}{\omega^2} \frac{1}{1 + 8 \ln^2(T\omega)^2} \quad (5)$$

in (4b) following directly from (3).

While the Hamiltonian (2) contains of course all dynamics implicitly, we aim at a formulation which brings out explicitly the relevant physical processes—light-induced shifts of the bound states, and non-adiabatic as well as  $n$ -photon induced electron transitions. We first construct a Hamiltonian

$$\mathcal{H}_{n_{\max}}(t) = -\frac{1}{2}\nabla^2 + \sum_{n=-n_{\max}}^{+n_{\max}} V_n(\mathbf{r}, t) e^{-in\omega t}, \quad (6a)$$

where the  $V_n(\mathbf{r}, t)$  are *single-cycle* averaged Fourier-components of the potential in (2),

$$V_n(\mathbf{r}, t) = \frac{1}{T_\omega} \int_0^{T_\omega} dt' V(\mathbf{r} + \mathbf{e}_x \alpha(t) \cos(\omega t' + \delta)) e^{in\omega t'}. \quad (6b)$$

Note, that (6) is *not* the usual Floquet representation which would absorb the entire time dependence in the Fourier phases  $e^{in\omega t}$  with time-independent coefficients  $V_n = V_n(\mathbf{r})$ . Yet, formally, it represents a faithful formulation of the full Hamiltonian in the limit  $n_{\max} \rightarrow \infty$ . What has been achieved with (6) is the separation of the time dependence due to the oscillatory electric field with carrier frequency  $\omega$  and due to the envelope of the short pulse, still contained in the time-dependent potentials  $V_n(\mathbf{r}, t)$ .

### 2.2. Minimal expansion length $n_{\max} = 2$

The expansion (6) is of course only useful, if a few terms (a few photons) are sufficient to describe the dynamics in question accurately. For weak pulses ( $\alpha_0 \rightarrow 0$ ) of any pulse duration the linear regime of single-photon absorption is approached suggesting  $n_{\max} = 1$  as the minimal expansion length. However, to achieve agreement of  $\mathcal{H}_{n_{\max}}$  with the full Hamiltonian for  $\alpha_0 \rightarrow 0$ , the expansion length  $n_{\max} = 2$  (maximally two-photon exchange) is required.

To see this we expand the single-cycle-averaged potentials  $V_n(\mathbf{r}, t)$  to 2nd order in  $\alpha_0$

$$V_0(\mathbf{r}, t) \approx V(\mathbf{r}) + \frac{1}{4} \frac{\partial^2 V}{\partial x^2} \alpha^2(t), \quad (7a)$$

$$V_{\pm 1}(\mathbf{r}, t) \approx \frac{1}{2} \frac{\partial V}{\partial x} \alpha(t) e^{\mp i\delta}, \quad (7b)$$

$$V_{\pm 2}(\mathbf{r}, t) \approx \frac{1}{8} \frac{\partial^2 V}{\partial x^2} \alpha^2(t) e^{\mp 2i\delta}, \quad (7c)$$

where  $\mathbf{r} = (x, y, z)$ . Inserted into equation (6a) the full potential without single-cycle averaging is recovered to order  $\alpha_0^2$ :

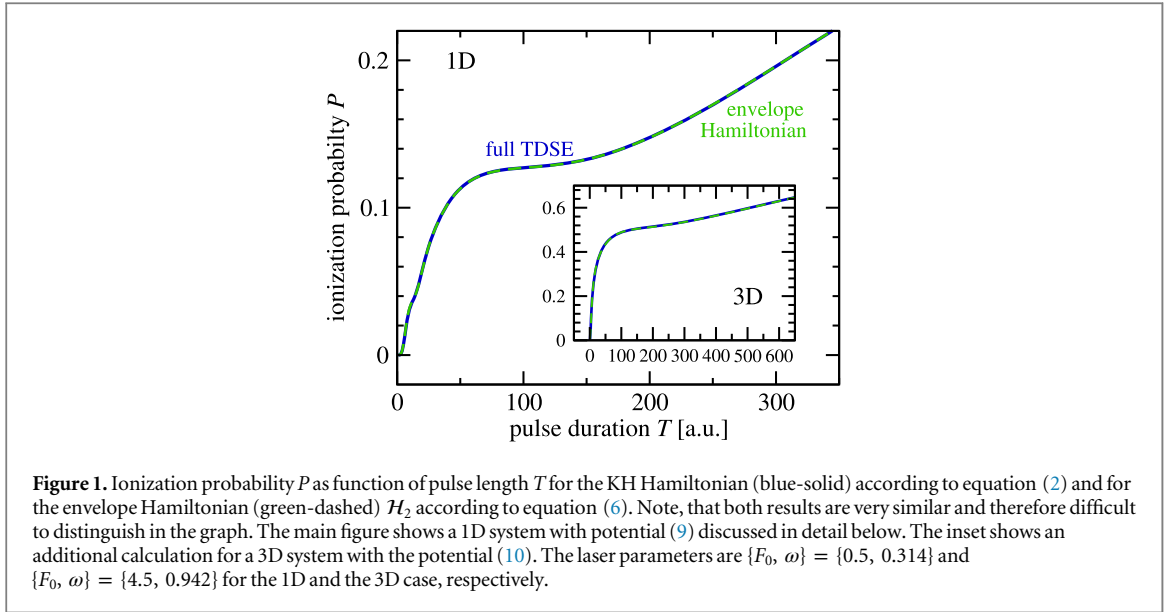


**Figure 1.** Ionization probability  $P$  as function of pulse length  $T$  for the KH Hamiltonian (blue-solid) according to equation (2) and for the envelope Hamiltonian (green-dashed)  $\mathcal{H}_2$  according to equation (6). Note, that both results are very similar and therefore difficult to distinguish in the graph. The main figure shows a 1D system with potential (9) discussed in detail below. The inset shows an additional calculation for a 3D system with the potential (10). The laser parameters are  $\{F_0, \omega\} = \{0.5, 0.314\}$  and  $\{F_0, \omega\} = \{4.5, 0.942\}$  for the 1D and the 3D case, respectively.

$$\begin{aligned} \sum_{n=-2}^{+2} V_n(\mathbf{r}, t) e^{-in\omega t} &\approx V(\mathbf{r}) + \frac{\partial V}{\partial x} \alpha(t) \cos(\omega t + \delta) + \frac{1}{2} \frac{\partial^2 V}{\partial x^2} \alpha^2(t) \cos^2(\omega t + \delta) \\ &\approx V(\mathbf{r} + \mathbf{e}_x \alpha(t) \cos(\omega t + \delta)). \end{aligned} \quad (8)$$

Since already the non-adiabatic term (7a) with zero-photon exchange contains the same interaction potential as the term (7c) with two-photon exchange, it is necessary to have a minimum expansion length of  $n_{\max} = 2$  in (6a) to achieve agreement with the full  $\mathcal{H}$  in the limit  $\alpha_0 \rightarrow 0$ . Therefore, we define the envelope Hamiltonian as  $\mathcal{H}_2$  in (6) with  $n_{\max} = 2$ . This implies physically, that  $\mathcal{H}_2$  describes correctly two extreme and seemingly opposite limits, namely very short and very long pulses. The latter is equivalently characterized by a large photon frequency or an optical period being short compared to the pulse duration  $T_\omega \ll T$ . Note that  $\mathcal{H}_2$  is sufficient for long pulses, even for large  $\alpha_0$ , since the continuum–continuum matrix elements are typically small.

### 2.3. Pulse-length dependent ionization from the envelope and the full Hamiltonian

Given that  $\mathcal{H}_2$  is exact for  $\alpha_0 \rightarrow 0$  it should also be a good approximation for finite  $\alpha_0$  as long as one photon takes a bound electron into the continuum. This is indeed the case as the following examples of a negative ion shows. It is described by a model potential [13]

$$V(x) = - \frac{\exp\left[-a_1 \sqrt{(x/a_1)^2 + a_2^2}\right]}{\sqrt{(x/a_1)^2 + a_3^2}} \quad (9)$$

with  $a_1 = 24.856$ ,  $a_2 = 0.16093$  and  $a_3 = 0.25225$ . With these parameters  $V(r)$  supports one bound state of energy  $\varepsilon_b = -0.0277$  a.u. Figure 1 shows the ionization probability as a function of pulse length with almost perfect agreement between the full dynamics (blue-solid) and the one obtained with the envelope Hamiltonian  $\mathcal{H}_2$  (green-dashed). The inset of figure 1 shows the same observable, however, calculated for a 3D system [14] with

$$V(\mathbf{r}) = -V_0 e^{-(|\mathbf{r}|/\tau_0)^2}, \quad (10)$$

where the parameters  $V_0 = 0.3831087$  and  $\tau_0 = 2.5026$  yield the same binding energy  $\varepsilon_b$  as in the 1D case. One sees the same excellent agreement of the full results with those obtained with  $\mathcal{H}_2$ .

This agreement is particularly astonishing for pulse lengths around the period of the bound electron<sup>1</sup>  $T_b = 69.1$  a.u., which represents exactly the dynamical regime we are targeting since the optical period is  $T_\omega = 20$  a.u., cf (1). Obviously, this match of time scales results in a plateau structure which we will explain below formulating an adiabatic time-dependent perturbation theory (aTDPT) for time-dependent basis functions. Although aTDPT is not necessary for using the envelope Hamiltonian  $\mathcal{H}_2$ , it allows one to work out and separate the mechanisms which lead to ionization with (6) in an intuitive way.

<sup>1</sup>We determine  $T_b$  from the classical period at the quantized energy  $\varepsilon_b$  of the respective bound state,  $T_b = \oint dx (2m/[\varepsilon_b - V(x)])^{1/2}$ .

### 3. Adiabatic time-dependent perturbation theory (aTDPT)

In fact, despite the presence of a strong field in terms of the ponderomotive energy the  $V_n$ ,  $|n| \geq 1$  can be treated as perturbations for suitable initial and final states, and aTDPT gives itself accurate quantitative results and simplifies the treatment of short pulses beyond the solution of  $\mathcal{H}_2$  since it requires only the solution of

$$\mathcal{H}_0(t) = -\frac{1}{2}\nabla^2 + V_0(\mathbf{r}, t), \quad (11)$$

while the other terms  $V_n$  in (6) can be treated perturbatively. We expand the wave function<sup>2</sup> into eigenstates  $|\beta(t)\rangle$  of  $\mathcal{H}_0(t)$  at fixed  $t$

$$|\psi\rangle = e^{-i\chi(t)} \sum_{\beta} c_{\beta}(t) |\beta(t)\rangle e^{-itE_{\beta}(t)}, \quad (12)$$

where  $|\beta(t)\rangle$  denotes both, bound and continuum eigenstates. The phase  $\chi(t)$  reflects the fact that eigenstates are defined up to a phase which can be time-dependent in our case and which is used to simplify the coupled differential equations for the coefficients  $c_{\beta}(t)$ . Details can be found in the appendix. In 1st-order time-dependent perturbation theory for the coefficients  $c_{\beta}$  and with initially only the bound state  $|b(t)\rangle$  occupied, i.e.  $c_b^{(0)}(t) = 1$  and  $c_{\beta \neq b}^{(0)}(t) = 0$ , the differential photo-ionization probability is given as usual by  $\frac{dP}{dk} = \lim_{t \rightarrow \infty} |c_k^{(1)}(t)|^2$ . With the envelope Hamiltonian  $\mathcal{H}_2$  the contributions to the cross section

$$\frac{dP}{dk} = \lim_{t \rightarrow \infty} \left| \sum_{n=-2}^2 M_n(\mathbf{k}, t) \right|^2 \quad (13a)$$

can be disentangled according to the number of photons  $n$  exchanged with  $\mathcal{H}_0(t)$  and described by the matrix elements

$$M_0(\mathbf{k}, t) = - \int_{-\infty}^t dt' \left\langle \mathbf{k}, t' \left| \frac{\partial}{\partial t'} \right| b(t') \right\rangle e^{i\phi_0(t')} \quad (13b)$$

and for one- and two-photon transitions,  $n = \pm 1, \pm 2$ ,

$$M_n(\mathbf{k}, t) = -i \int_{-\infty}^t dt' \langle \mathbf{k}, t' | V_n(\mathbf{r}, t') | b(t') \rangle e^{i\phi_n(t')} \quad (13c)$$

with the phases

$$\phi_n(t) = [k^2/2 - E_b(t) - n\omega]t. \quad (13d)$$

While equation (13a) looks familiar on a first glance, it exhibits clear differences compared to standard TDPT: without an explicit time-dependence of the basis functions  $|\beta(t)\rangle$ , the matrix element for non-adiabatic transitions (13b) vanishes. A bit more subtle is the energy difference in the phases  $\phi_n$ : while the energy characterizing the final ionized state is not time-dependent,  $E_{\beta} = \epsilon_k = k^2/2$ , the energy of the initial bound state is actually a time average  $E_b(t) = t^{-1} \int_{-\infty}^t dt' \epsilon_b(t')$  while  $[\mathcal{H}_0(t) - \epsilon_b(t)]|b(t)\rangle = 0$ .

### 4. Contributions to the ionization yield from the perspective of aTDPT

We will now analyze the pulse-length dependent ionization yield of figure 1 in more detail and concentrate for simplicity on the 1D case. As it turns out, the plateau-like shape of the ionization yield can be understood as a direct consequence of the pulse-length dependent behaviour of the different contributions  $M_n$  to the cross section, as illustrated in figure 2, which takes a closer look on the ionization dynamics, including the photo-electron spectrum for a pulse length of  $T = 100$  a.u. in figure 2(b). Although it represents a more differential property as compared to the total ionization yield, the same good agreement between the full dynamics and that of the envelope Hamiltonian can be seen.

The non-adiabatic contribution to the ionization probability  $P_0 \equiv \int \frac{dk}{2\pi} |M_0(k, \infty)|^2$ , is shown in figure 2 (blue-dotted line). It becomes substantial for  $T < T_b$ , i.e., when the pulse length is shorter than the period of the electron. As a consequence, the electron cannot follow the pulse anymore and undergoes non-adiabatic transitions leading to accumulation of amplitude in the continuum. On the other hand for  $T > T_b$  the electron dynamics is adiabatic and  $M_0$  does not lead to ionization. The SPI described by  $P_1 = \int \frac{dk}{2\pi} |M_1(k, \infty)|^2$  is due to  $V_1$  and grows linearly for large  $T$  in accordance with a single-photon process. The total ionization probability reached is no longer small compared to unity and depletion of the ground state must be taken into account,

<sup>2</sup>The expansion of the time-dependent wavefunction in adiabatic states has been proposed first by Born and Fock [15].

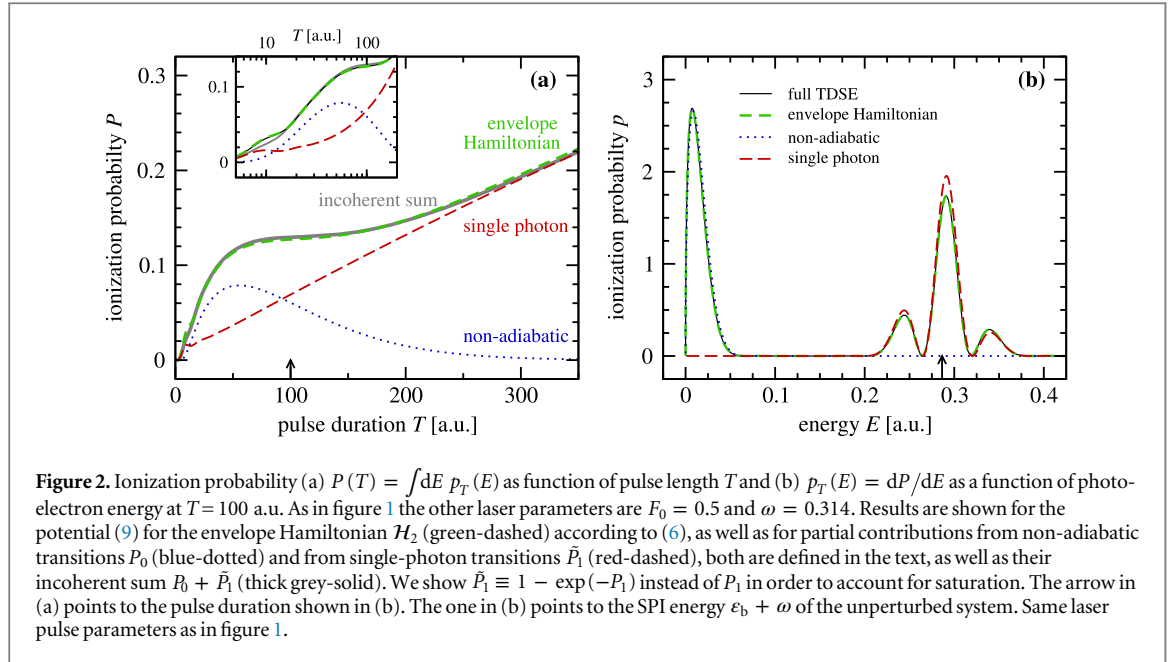


**Figure 2.** Ionization probability (a)  $P(T) = \int dE p_T(E)$  as function of pulse length  $T$  and (b)  $p_T(E) = dP/dE$  as function of photo-electron energy at  $T = 100$  a.u. As in figure 1 the other laser parameters are  $F_0 = 0.5$  and  $\omega = 0.314$ . Results are shown for the potential (9) for the envelope Hamiltonian  $H_2$  (green-dashed) according to (6), as well as for partial contributions from non-adiabatic transitions  $P_0$  (blue-dotted) and from single-photon transitions  $\tilde{P}_1$  (red-dashed), both are defined in the text, as well as their incoherent sum  $P_0 + \tilde{P}_1$  (thick grey-solid). We show  $\tilde{P}_1 \equiv 1 - \exp(-P_1)$  instead of  $P_1$  in order to account for saturation. The arrow in (a) points to the pulse duration shown in (b). The one in (b) points to the SPI energy  $\varepsilon_b + \omega$  of the unperturbed system. Same laser pulse parameters as in figure 1.

leading to  $P_1 \rightarrow \tilde{P}_1 \equiv 1 - \exp(-P_1)$  and shown as red-dashed line in figure 2. Remarkably, the *incoherent* sum of both probabilities  $P_0 + \tilde{P}_1$  (thick grey-solid line in figure 2(a)) approximates very accurately the full ionization probability  $P(T)$  from the coherent superposition of amplitudes (13a) (green-dashed in figure 2(a)). Typically, this is the case if the differential probabilities  $dP_n/dk = |M_n(k, \infty)|^2$  peak at very different momenta  $k$  such that the overlap integrals  $\int dk M_n^*(k, \infty) M_m(k, \infty)$  for  $n \neq m$  vanish.

This is indeed the case, as the photo-electron spectrum in figure 2(b) reveals: non-adiabatic transitions produce low-energy electrons [16] whose probability  $dP_0/dE$  (blue-dotted) is well separated from the contribution  $d\tilde{P}_1/dE$  (red-dashed) mainly due to single-photon absorption. The latter peaks close but not at the CW laser photo-line at  $E = \varepsilon_b(-\infty) + \omega = 0.2864$ . This is the result of two competing effects. Firstly, there is a red-shift due to the finite width of the SPI peak which is convoluted with the exponentially decreasing dipole matrix element in (13c). Secondly, there are the well-known light-induced shifts of the energy levels, notably the initial bound state  $\varepsilon_b$  gets lifted upwards leading to a blue-shift of the SPI peak. In the limit of  $\omega T \gg 1$  the red-shift disappears, while the blue-shift is only influenced by the quiver amplitude.

The SPI peak does not only shift if generated by an intense short pulse, it also gets modulated as a result of interference of photo-electron emission in the rising and falling wing of the pulse [17, 18] recently also found in molecules [19, 20] and termed *dynamic* interference. *Spatial* interference, i.e. ionization from different position of the oscillating potential [9], during the peak of the pulse can be interpreted as the onset of stabilization. However, formulating the ionization yield—a quantity naturally defined at asymptotically long times—during the laser pulse is an intricate problem, which can easily be solved by defining cycle-averaged ionization yields.

#### 4.1. Pulse-dependent photo-ionization rates

The adiabatic perturbation theory for parametrically time-dependent perturbations suggests to formulate photo-ionization rates (involving true photon absorption) *during* the laser pulse as photo-ionization rates per optical cycle. To this end we simply define the probability for SPI (here for clarity in the 1D case) at time  $t$  by integrating the single-photon transition matrix element  $M_n(k, t)$  over energy and an arbitrary number  $N$  of laser periods  $T_\omega$

$$P_n(t) = \int \frac{dk}{2\pi} \left| \int_0^{NT_\omega} dt' \langle k, t | V_n(x, t) | b(t) \rangle e^{it' [k^2/2 - n\omega - \varepsilon_\beta(t)]} \right|^2, \quad (14)$$

where we have fixed all pulse-envelope related time dependencies including that of the bound state energy  $\varepsilon_b$  as a parameter. Then  $E_b(t) = \varepsilon_b(t)$ , since  $E_b(t') \approx [1/t'] \int_0^{t'} dt'' \varepsilon_b(t'') = \varepsilon_b(t)$ . For large  $N$  the residual time dependence  $t'$  in the phase of the integral in (14) produces a  $\delta$ -function  $2\pi\delta(k^2/2 - n\omega - \varepsilon_b(t))$  while the second (complex conjugate) integral gives then trivially  $NT_\omega$ . The final result for the SPI rate is then

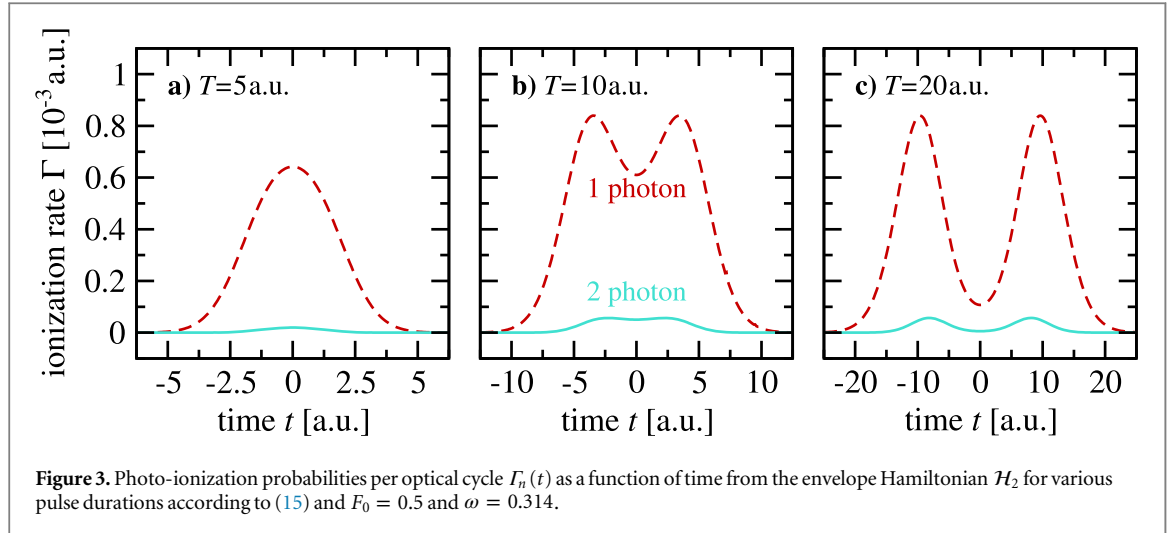


**Figure 3.** Photo-ionization probabilities per optical cycle  $\Gamma_n(t)$  as a function of time from the envelope Hamiltonian  $\mathcal{H}_2$  for various pulse durations according to (15) and  $F_0 = 0.5$  and  $\omega = 0.314$ .

$$\Gamma_n(t) = \frac{P_n(t)}{NT_\omega} = \frac{1}{k} \left( \left| \langle +k(t) | V_n(x, t) | b(t) \rangle \right|^2 + \left| \langle -k(t) | V_n(x, t) | b(t) \rangle \right|^2 \right) \quad (15)$$

with  $k(t) = [2n\omega + 2\varepsilon_b(t)]^{1/2}$ . Similarly, one can proceed for  $n$ -photon ionization rates and the results for one- and two-photon transition probabilities  $M_n$ ,  $n = 1, 2$  are shown in figure 3. For sufficiently large quiver amplitude of the classical trajectory (4)—varied with the help of the pulse length, see (5)—a double-hump structure appears corresponding to two distinct maximal ionization probabilities before and after the pulse maximum. The intermittent decrease of the ionization probability leading to this double hump is a signature of stabilization around the maximum of the laser pulse.

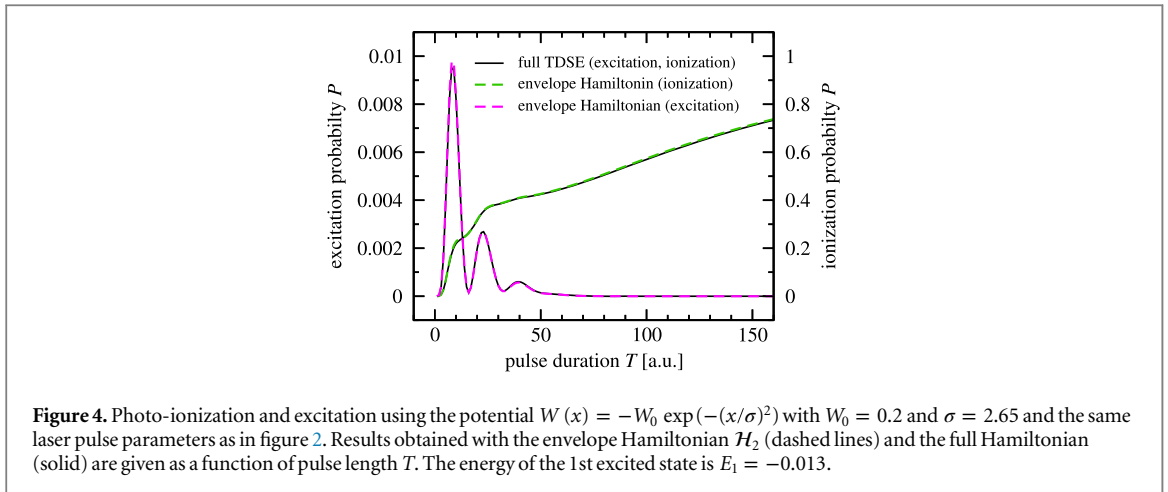
It affects single- as well as multi-photon ionization as can be seen in figure 3 but requires a large enough pulse amplitude and therefore does not occur for  $T = 5$ . Figure 3 also illustrates, why the envelope Hamiltonian is such a good approximation: two-photon ionization (green line) does happen, but is already quite small, such that  $n$ -photon absorption with  $n \geq 3$  can be neglected. The reason is not a weak field—in fact the ponderomotive energy for  $T$  being large is with 0.63 a.u. quite large compared to the binding energy  $E_b \approx 0.03$  a.u. Small, however, is the probability for absorption of a (subsequent) photon in the continuum which is required for multi-photon absorption. This explains, why terms  $V_n$  up to  $n = 2$  are sufficient to capture the full dynamics. Of course, separating off the time dependence of the laser envelope is crucial: if this is not done, all time dependence is contained in the Fourier amplitudes  $e^{in\omega t}$ . In this case an expansion to  $n$  much larger than the number of absorbed photons is necessary to capture a fast changing envelope.

While the modulation, seen in figure 2 and described in detail elsewhere [17, 18], occurs due to interference within the single-photon contribution  $|M_1|^2$ , there is also an effect due to the coherence between the SPI and the non-adiabatic amplitude, but only for pulse lengths comparable or shorter than the optical period  $T_\omega$ , where the SPI peak becomes very broad and starts to overlap with the non-adiabatic electron peak (see inset of figure 2(a)).

## 5. Summary and outlook

We have formulated a systematic separation of the time-dependence of the dynamics of an electron, bound to a target and subject to a short, intense light pulse. By Fourier expanding the electron's potential in the KH frame with a single optical cycle as support in the time-domain, we have obtained time dependent potentials  $V_n(\mathbf{r}, t)$ ,  $n = 0, \pm 1, \pm 2, \dots$  as Fourier components which reflect  $n$ -photon exchange processes. Based on formal considerations of agreement with the exact Hamiltonian for small quiver amplitudes  $\alpha_0$ , we have defined the envelope Hamiltonian  $\mathcal{H}_2$  as promising approximation containing the  $V_n$  up to  $|n| \leq 2$ . We tested  $\mathcal{H}_2$  on a single active electron in negative ion in one and three-dimensions and have seen that  $\mathcal{H}_2$  provides not only an excellent description for  $\alpha_0 \ll 1$ , but also of electron dynamics for pulses with  $T/T_\omega \sim 1$  and  $\alpha_0 > 1$ , where neither the small  $\alpha_0$  expansion can justify the envelope Hamiltonian, nor an adiabatic variation of the pulse envelope ( $T/T_\omega \gg 1$ ). For the parameters of figure 2(a) with  $F_0 = 0.5$  and  $T_\omega = 20$  this situation corresponds to pulse lengths from about 3 a.u. ( $\alpha_0 = 1.12$ ) to 200 a.u. ( $T/T_\omega \sim 10$ ).

One may of course ask, if the excellent quantitative and qualitative description of the short-pulse ionization dynamics provided by the envelope Hamiltonian is restricted to the potential (9) for which it has been demonstrated here—which, for technical reasons was chosen to be short-range (negative ion) which also implies for our choice that there is only one bound state. For this reason, we present in figure 4 the result for a



Gaussian binding potential of the form  $W(x) = -W_0 \exp(-(x/\sigma)^2)$  whose parameters with a ground state of  $\epsilon_b = -0.1$  and corresponding electron period of  $T_b = 34.1$  have been chosen such that the hierarchy of time scales (1) is fulfilled with the same laser pulse we have been using for  $V(x)$  from (9). The potential  $W$  supports in contrast to  $V$  also an excited state which is indeed also populated during the laser pulse interaction. Again, the description with the envelope Hamiltonian is almost perfect. We have done similar calculation for other scenarios with short range Hamiltonians always finding excellent agreement with the full numerical solution. We expect our approach to be equally accurate for long range potentials. The formulation of the envelope Hamiltonian itself does not make any use of dimensionally restricted dynamics. Moreover, we have seen that the incoherent superposition of non-adiabatic and SPI probabilities relies on the fact that both processes peak at different photo-electron momenta rendering the overlap integral of the respective amplitudes small. This effect will be eventually amplified but certainly not diminished when full 3D dynamics is considered. If the non-adiabatic contribution is equally important for realistic parameters of the light in 3D situations—leading to plateau-like structures in the ionization yield—remains to be seen in future studies.

So far the time-dependence for the envelope of the laser pulse in a Fourier representation of the KH Hamiltonian has been proposed only for adiabatically slowly varying envelopes in the literature [16], where this is a natural ansatz. In this work, we have formulated an envelope Hamiltonian and applied it successfully to the opposite limit, namely envelopes which vary fast as compared to the optical cycle and even the natural time scale of the bound electron. The success of the envelope Hamiltonian has two roots: firstly, with the time-dependent Floquet formulation of (6) different photo processes can be separated according to the number of photons absorbed: from non-adiabatic transitions requiring no photons (only a fast changing laser envelope) to single or eventually multiple photon ionization contributions. Thereby, each photon leads to a blue-shift of the spectral appearance of the corresponding photo electrons by  $\omega$ , separating the contributions well in energy for pulses not too short. Secondly, despite the strong field two- and more-photon absorption is unlikely since it has to happen in the continuum. This allows for the formulation of a perturbation theory in the number of absorbed photons based on (6).

Complementary to a full time-dependent numerical solution, the present work offers a Hamiltonian whose different interaction parts represent  $n$ -photon transitions (as one is used to for longer laser pulses) and in addition a new interaction which contains non-adiabatic transitions due to the short pulse length. Many applications of the envelope Hamiltonian for quite different physical scenarios fulfilling the hierarchy of time scales (1) are feasible. Given the lack of accurate approximations for the electron dynamics under ultrashort pulses, attosecond pulse interaction appears particularly attractive for aTDPT with the envelope Hamiltonian as introduced here. Apart from offering an alternative for a numerical treatment it offers an transparent interpretation of ultra-fast light-matter coupling.

## Acknowledgments

This work was supported by the COST Action XLIC (CM 1204) and the Marie Curie Initial Training Network CORINF.

## Appendix

Here, we sketch the general formulation of an aTDPT for  $\mathcal{H} = \mathcal{H}_0(t) + U(x, t)$ , split into an unperturbed Hamiltonian

$$\mathcal{H}_0(t) = -\frac{1}{2}\nabla^2 + V_0(\mathbf{r}, t), \quad (\text{A.1})$$

which is itself parametrically time-dependent and a time-dependent perturbation  $U(\mathbf{r}, t)$ . Let  $|j(t)\rangle$  and  $|\mathbf{k}, t\rangle$  be an eigenstate of the Hamiltonian  $\mathcal{H}_0(t)$  for fixed time  $t$  from the discrete and continuous part of the spectrum, respectively

$$\mathcal{H}_0(t)|j(t)\rangle = |j(t)\rangle \varepsilon_j(t) \quad (\text{A.2a})$$

$$\mathcal{H}_0(t)|\mathbf{k}, t\rangle = |\mathbf{k}, t\rangle \varepsilon_{\mathbf{k}} \quad \text{with} \quad \varepsilon_{\mathbf{k}} = \frac{\mathbf{k}^2}{2}. \quad (\text{A.2b})$$

Together the  $|j(t)\rangle$  and  $|\mathbf{k}, t\rangle$  form a complete orthonormal basis set

$$\langle j(t)|j'(t)\rangle = \delta_{jj'}, \quad \langle j(t)|\mathbf{k}, t\rangle = 0, \quad \langle \mathbf{k}, t|\mathbf{k}', t\rangle = (2\pi)^3 \delta(\mathbf{k} - \mathbf{k}'), \quad (\text{A.3})$$

which we label in the following for simplicity with greek letters. Consequently  $\sum_{\beta} |\beta(t)\rangle \langle \beta(t)| = 1$  holds. Note that the eigenenergies  $\varepsilon_j(t)$  as well as all basis functions are time-dependent but the continuum energies  $\varepsilon_{\mathbf{k}} = \mathbf{k}^2/2$  of course not.

We expand the solution  $\psi(t)$  of the Schrödinger equation

$$[\mathcal{H}_0(t) + Q(\mathbf{r}, t)]|\psi(t)\rangle = 0 \quad \text{with} \quad Q(\mathbf{r}, t) \equiv U(\mathbf{r}, t) - i\partial/\partial t \quad (\text{A.4})$$

as

$$|\psi(t)\rangle = e^{-i\chi(t)} \sum_{\beta} |\beta(t)\rangle c_{\beta}(t) e^{-itE_{\beta}(t)}, \quad (\text{A.5})$$

where  $\chi(t)$  is the usual phase freedom which is in our case time-dependent and will be chosen later to obtain a simple form of the differential equations for the coefficients  $c_{\beta}$ . For continuum states  $\beta = \mathbf{k}$  we have  $E_{\mathbf{k}}(t) \equiv \varepsilon_{\mathbf{k}}$  as usual, but for the bound states  $\beta = j$  the energies for the phase factor are given by  $E_j(t) \equiv t^{-1} \int^t dt' \varepsilon_j(t')$ .

If we insert the ansatz (A.5) into (A.4) and project from the left onto  $|\beta\rangle$  we obtain

$$i \dot{c}_{\beta}(t) = -c_{\beta}(t) \dot{\chi}(t) + \sum_{\beta'} Q^{\beta\beta'}(t) c_{\beta'}(t) e^{-it[E_{\beta'}(t) - E_{\beta}(t)]}, \quad (\text{A.6a})$$

where

$$Q^{\beta\beta'}(t) \equiv \langle \beta(t)|Q(\mathbf{r}, t)|\beta'(t)\rangle \quad (\text{A.6b})$$

with  $Q$  from (A.4).

The coupled equations A.6a provide a full solution to (A.4). However, if  $U(x, t)$  is only a weak perturbation, we can solve (A.4) to a good approximation by a single iteration, where we assume that only 1st-order transitions (linear in  $U$  or in  $Q$ , respectively) occur. With an initial occupation of a bound state  $|b\rangle$  and all other states unoccupied it is

$$c_b^{(0)}(t) = 1, \quad c_{\beta \neq b}^{(0)}(t) = 0, \quad (\text{A.7})$$

and we obtain by a single iteration of (A.6a)

$$i \dot{c}_b^{(1)}(t) = [Q^{bb}(t) - \dot{\chi}(t)] c_b^{(0)}(t) + \sum_{\beta \neq b} Q^{b\beta}(t) c_{\beta}^{(0)}(t) e^{-it[E_{\beta}(t) - E_b(t)]} \quad (\text{A.8a})$$

$$i \dot{c}_{\beta}^{(1)}(t) = -\dot{\chi}(t) c_{\beta}^{(0)}(t) + Q^{\beta b}(t) c_b^{(0)}(t) e^{-it[E_b(t) - E_{\beta}(t)]} + \sum_{\beta' \neq b} Q^{\beta\beta'}(t) c_{\beta'}^{(0)}(t) e^{-it[E_{\beta'}(t) - E_{\beta}(t)]}. \quad (\text{A.8b})$$

If we choose  $\dot{\chi} = Q^{bb}$  we obtain from (A.8a)  $\dot{c}_b^{(1)}(t) = 0$  implying  $c_b^{(1)}(t) = c_b^{(0)}(t) = 1$  and from (A.8b) for  $\beta \neq b$

$$c_{\beta}^{(1)}(t) = -i \int_{-\infty}^t dt' Q^{\beta b}(t') e^{-it'[E_b(t') - E_{\beta}(t')]}. \quad (\text{A.9})$$

The result (A.9) of this aTDPT agrees formally with that of the standard TDPT except for two (subtle) differences: (i) the basis states entering the matrix element  $Q^{\beta\beta'}$ , cf (A.6b), are explicitly time-dependent and (ii) so are the energies  $E_{\beta}(t)$  for the bound states, e.g.,  $\beta = b$ .

The lowest-order (time-dependent) correction to the bound states is  $\mathcal{O}(\alpha_0^2)$ , where  $\alpha_0$  is the effective quiver amplitude (5). Taking only terms up to order  $\alpha_0$  we get

$$\tilde{c}_\beta(t) = -i \int_{-\infty}^t dt' \langle \beta | U(\mathbf{r}, t') | b \rangle e^{-i(E_b - \epsilon_\beta)t'}, \quad (\text{A.10})$$

which coincides with the result of standard TDPT in textbooks. In general, the population of a state  $|\beta(t)\rangle$  at any time  $t$  is given in a TDPT by (A.9), provided that the system was initially in state  $|b\rangle$ .

## References

- [1] Blaga C I, Catoire F, Colosimo P, Paulus G G, Müller H G, Agostini P and di Mauro L F 2009 *Nat. Phys.* **5** 335
- [2] Quan W *et al* 2009 *Phys. Rev. Lett.* **103** 093001
- [3] Kästner A, Saalman U and Rost J-M 2012 *Phys. Rev. Lett.* **108** 033201  
Kästner A, Saalman U and Rost J-M 2012 *J. Phys. B: At. Mol. Opt. Phys.* **45** 074011
- [4] Lemell C, Dimitriou K I, Tong X-M, Nagele S, Kartashov D V, Burgdörfer J and Gräfe S 2012 *Phys. Rev. A* **85** 011403
- [5] Førre M, Selstø S, Hansen J P and Madsen L B 2005 *Phys. Rev. Lett.* **95** 043601
- [6] Toyota K, Tolstikhin O I, Morishita T and Watanabe S 2009 *Phys. Rev. Lett.* **103** 153003
- [7] Gavrilin M and Kamiński J 1984 *Phys. Rev. Lett.* **52** 613
- [8] Henneberger W C 1968 *Phys. Rev. Lett.* **21** 838
- [9] Gavrilin M 2002 *J. Phys. B: At. Mol. Opt. Phys.* **35** R147
- [10] Popov A M, Tikhonova O V and Volkova E A 2003 *J. Phys. B: At. Mol. Opt. Phys.* **36** R125
- [11] Morales F, Richter M, Patchkovskii S and Smirnova O 2011 *Proc. Natl Acad. Sci. USA* **108** 16906
- [12] Joachain C J, Kylstra N J and Potvliege R M 2011 *Atoms in Intense Laser Fields* (Cambridge: Cambridge University Press)
- [13] Grobe R and Eberly J H 1993 *Phys. Rev. A* **47** 719
- [14] Toyota K, Tolstikhin O I, Morishita T and Watanabe S 2008 *Phys. Rev. A* **78** 033432
- [15] Born M and Fock V 1928 *Z. Phys.* **51** 165
- [16] Barash D, Orel A E and Baer R 1999 *Phys. Rev. A* **61** 013402
- [17] Toyota K, Tolstikhin O I, Morishita T and Watanabe S 2007 *Phys. Rev. A* **76** 043418
- [18] Demekhin P V and Cederbaum L S 2012 *Phys. Rev. Lett.* **108** 253001
- [19] Yu C, Fu N, Hu T, Zhang G and Yao J 2013 *Phys. Rev. A* **88** 043408
- [20] Yue L and Madsen L B 2014 *Phys. Rev. A* **90** 063408